



The Catalytic Role of RuBisCO for *in situ* CO₂ Recycling in *Escherichia coli*

Ju-Jiun Pang¹, Jong-Shik Shin² and Si-Yu Li^{1,3*}

¹ Department of Chemical Engineering, National Chung Hsing University, Taichung City, Taiwan, ² Department of Biotechnology, Yonsei University, Seoul, South Korea, ³ Innovation and Development Center of Sustainable Agriculture, National Chung Hsing University, Taichung City, Taiwan

OPEN ACCESS

Edited by:

Ranieri Cancedda,
Independent Researcher, Genoa, Italy

Reviewed by:

Peter Lindblad,
Uppsala University, Sweden
Min Jiang,
Nanjing Tech University, China

*Correspondence:

Si-Yu Li
syli@dragon.nchu.edu.tw

Specialty section:

This article was submitted to
Synthetic Biology,
a section of the journal
Frontiers in Bioengineering and
Biotechnology

Received: 18 March 2020

Accepted: 13 October 2020

Published: 30 November 2020

Citation:

Pang J-J, Shin J-S and Li S-Y
(2020) The Catalytic Role of RuBisCO
for *in situ* CO₂ Recycling
in *Escherichia coli*.
Front. Bioeng. Biotechnol. 8:543807.
doi: 10.3389/fbioe.2020.543807

Ribulose-1,5-bisphosphate carboxylase/oxygenase (RuBisCO) is a key enzyme responsible for biological CO₂ assimilation. RuBisCO can be heterologously expressed in *Escherichia coli* so that glucose and CO₂ are co-metabolized to achieve high mixotrophic metabolite production, where the theoretical yield of mixotrophic metabolite production is 2.4 mol_(ethanol+acetate+pyruvate)/mol_{glucose}. However, RuBisCO is known for its low k_{cat} and for forming inhibited complexes with its substrate ribulose-1,5-bisphosphate (RuBP) and other sugar phosphates, yet the inhibited form of RuBisCO can be reversed by RuBisCO activase (Rca). In this study, RuBisCO forms I and II were cloned and expressed in *Escherichia coli* for *in situ* CO₂ recycling, where CO₂ produced during glucose fermentation was recycled and co-metabolized with the glucose. In addition, forms I and II RuBisCO activases were co-expressed with RuBisCO in *E. coli* to determine their *in vivo* effects on *in situ* CO₂ recycling. Form I RuBisCO activase (Rca1) was co-expressed with form I RuBisCO and form II RuBisCO activase (Rca2) was co-expressed with form II RuBisCO. The results showed that both form I and form II RuBisCO exhibit comparable activities in *E. coli* and generated similar levels of *in situ* CO₂ recycling. A significant increase in the total metabolite yield from 1.5 ± 0.1 to 2.2 ± 0.1 mol_(ethanol+acetate+pyruvate)/mol_{glucose} occurred when Rca2 was co-expressed with form II RuBisCO. Meanwhile, the total metabolite yield increased from 1.7 ± 0.1 to 2.0 ± 0.1 mol_(ethanol+acetate+pyruvate)/mol_{glucose} when Rca1 was co-expressed with form I RuBisCO. This data suggests that both forms I and II RuBisCO are subject to *in vivo* RuBP inhibition yet can be relieved by the co-expression of Rca. Interestingly, it is suggested that the *in vivo* RuBP inhibition of form II RuBisCO can be more easily reversed compared to form I. When the catalytic power of RuBisCO is maintained by Rca, the high activity of phosphoribulokinase (Prk) plays an important role in directing glucose to the RuBisCO-based engineered pathway and fermentation yields of 2.1–2.3 mol_(ethanol+acetate+pyruvate)/mol_{glucose} can be obtained. This study is the first to demonstrate that *in vivo* RuBP inhibition of RuBisCO can be a bottleneck for *in situ* CO₂ recycling in *E. coli*.

Keywords: Carbon dioxide, mixotroph, Ribulose-1,5-bisphosphate carboxylase/oxygenase, RuBisCO activase, *Acidithiobacillus ferrooxidans*

Abbreviations: RuBisCO, Ribulose-1,5-bisphosphate carboxylase/oxygenase; RuBP, ribulose-1,5-bisphosphate; Rca, RuBisCO activases; CBB cycle, Calvin-Benson-Bassham (CBB) cycle.

INTRODUCTION

The Calvin-Benson-Bassham (CBB) cycle is one of the main metabolic pathways for converting inorganic CO₂ to organic carbon during photosynthesis (Tabita et al., 2008; Nielsen et al., 2012; François et al., 2020). Ribulose-1, 5-bisphosphate carboxylase/oxygenase (RuBisCO) is a key enzyme of the CBB cycle and is responsible for CO₂ fixation by catalyzing the carboxylation of RuBP. RuBisCO can be categorized into four groups: form I, II, III, and IV (Badger and Bek, 2008). These four different forms are structurally unique (Tabita et al., 2008). However, to date, only forms I and II RuBisCO have proven to operate in the CBB cycle (Tabita et al., 2008). The first RuBisCO structure determined by X-ray crystallography was from the bacterium *Rhodospirillum rubrum*, which is now categorized as form II (Tabita et al., 2008). This enzyme is composed of only two large subunits (L₂) which share 25–30% identity to the L subunits of form I RuBisCO. Form II RuBisCO is considered to be an original form of RuBisCO (Tabita et al., 2008), and the catalytic site is at the interface between the L subunits. Conversely, form I RuBisCO is composed of eight L subunits (~53 kDa) and eight small (S) subunits (~15 kDa). The basic structural motif, dimer of L, is repeated four times to form a catalytic (L₈) core with eight S subunits capping the top and the bottom of this core (Tabita et al., 2008). Similarly, the catalytic site of form I RuBisCO is also at the interface between the L subunits. In addition, based on phylogenetic analysis of the amino acid sequence, form I RuBisCO can be further classified as red-like and green-like RuBisCO. Form I RuBisCO is the most abundant enzyme on Earth and can be found in eukaryotes, bacteria, and higher plants (Ashida et al., 2008).

The catalytic activity of RuBisCO requires an activation step. First, non-substrate CO₂ binds to an active site to convert the conserved Lys²⁰¹ to a carbamylated form, which is then stabilized by Mg²⁺. As a result, the activated form of RuBisCO is capable of converting substrate RuBP and CO₂ into two molecules of 3-phosphoglycerate (PGA). In contrast, the binding of RuBP to a decarbamylated enzyme prior to CO₂ leads to a dead-end complex in which activation requires an energy-consuming conformational change of RuBisCO to release the bound RuBP (Parry et al., 2008). RuBisCO is prone to forming inactive complexes; therefore, the activation of RuBisCO is critical for catalysis (McNevin et al., 2006). RuBisCO is also known to be inhibited by other sugar phosphates, such as xylulose-1,5-bisphosphate and 2,3-pentodiulose-1,5-bisphosphate (Parry et al., 2008).

RuBisCO activase (Rca) is known to mediate the release of the inhibitory sugar phosphate from the inactive RuBisCO. It was identified as a biochemical lesion responsible for the high CO₂-requiring phenotype of the Rca mutant of *Arabidopsis* (Somerville et al., 1982), which lacks the Rca protein (Salvucci et al., 1985). A previous study showed that RuBisCO cannot achieve and maintain an adequate level of activity for growth at ambient CO₂ without the aid of Rca (McNevin et al., 2006). Rca reactivates RuBisCO by consuming ATP and therefore belongs to the AAA+ superfamily (ATPases associated with diverse cellular activities). Three classes of Rca have been characterized (Mueller-Cajar, 2017). The first class acts on plants whereas the

second class (known as CbbX) acts on bacterial red-type form I RuBisCO. In a recent study, a third class of Rca (named CbbQO type Rca) found in a chemolithoautotroph *Acidithiobacillus ferrooxidans* (ATCC 23270) was biochemically characterized (Tsai et al., 2015). Two isoforms of CbbQO protein complexes, form I Rca (Rca1) and form II Rca (Rca2), *in vitro* elevate the activities of forms I and II RuBisCO, respectively, where CbbQ acts as a motor to catalyze ATP hydrolysis and CbbO acts as a functional binder to interact with RuBisCO (Tsai et al., 2015). The native quaternary structure of Rca (Q₆O₁) has been classified as a MoxR AAA+ ATPase, where CbbQs form a hexameric ring-shaped conformation. A recent structural and biochemical study has been shown that the axial pore of the hexameric CbbQ ring is critical for CbbQ docking and consequently executing ATPase activity (Tsai et al., 2020). The side of the hexameric CbbQ ring is essential for RuBisCO binding and docking (Tsai et al., 2020).

The partial Calvin cycle was constructed in *Escherichia coli* where phosphoribulokinase (Prk) and RuBisCO (originating from *Synechococcus* PCC6301) were heterologously expressed for directed evolution of RuBisCO (Parikh et al., 2006). Then, the partial Calvin cycle in *E. coli* was investigated for *in situ* CO₂ recycling during the fermentation of pentoses (Zhuang and Li, 201) and hexose (Li et al., 2015; Yang et al., 2016). Recently, a study showed that this RuBisCO-based engineered *E. coli* [*E. coli* MZLFB (BL21(DE3) Δ zwf Δ ldh Δ frd, harboring three genes (*rbcL*, *rbcS*, and *prk*) surpassed the conventional yield of 2 mol_(ethanol+acetate+pyruvate)/mol_{glucose} to reach 2.2 mol_(ethanol+acetate+pyruvate)/mol_{glucose} (Tseng et al., 2018). This mixotrophic fermentation, where sugar and CO₂ are simultaneously assimilated for fermentation production, leads to a theoretical yield of fermentation products of 2.4 mol_(ethanol+acetate+pyruvate)/mol_{glucose}.

Although functional expression of RuBisCO in *E. coli* (Parikh et al., 2006; Tsai et al., 2015; Antonovsky et al., 2016; Tseng et al., 2018) and yeast (Gassler et al., 2019) have been reported, the low k_{cat} of RuBisCO raises the question of how the catalytic performance of RuBisCO affects the rate of CO₂ fixation. In this study, the effect of forms I and II RuBisCOs from *A. ferrooxidans* (ATCC 23270) on the rate of *in situ* CO₂ recycling in the RuBisCO-based engineered *E. coli* was investigated. Moreover, the third and newly disclosed class of Rca, RcaQ1O1 (encoded by *cbbQ1* and *cbbO1*, designated as Rca1 in this study) and RcaQ2O2 (encoded by *cbbQ2* and *cbbO2*, designated as Rca2 in this study), from *A. ferrooxidans* (ATCC 23270) (Tsai et al., 2015), were cloned and expressed in RuBisCO-based engineered *E. coli*. The *in vivo* effects of Rca on the regulation of RuBisCO activity were investigated for the first time by monitoring its rate of *in situ* CO₂ recycling. The conjugation of form I RuBisCO-Rca1 or form II RuBisCO-Rca2, which are all from *A. ferrooxidans*, was tested in the RuBisCO-based engineered *E. coli*. To demonstrate the generality of this approach, the *in vivo* interaction of Rca1 with form I RuBisCO from a different organism, *Synechococcus* PCC6301 (*rbcLS*), was also investigated. *RbcLS* lacks the HK/R motif at the C-terminus of the large subunit, where the HK/R motif of form I RuBisCO from *A. ferrooxidans* (AfcbbLS) was proposed to be important for the *in vitro* interaction of AfcbbLS and Rca1 (Tsai et al., 2015). The role of the HK/R motif in the *in vivo* interaction between *rbcLS* and Rca1 was investigated.

MATERIALS AND METHODS

Bacterial Strains and Plasmids

All strains and plasmids used in this study are listed in **Table 1**.

Construction of Recombinant Plasmids

The RuBisCO genes *cbmM* (AFE_2155) were amplified from pHueAfcbbM (Tsai et al., 2015) and cloned between the *NcoI*-*XbaI* sites of the vector *rbclS*-pET30a(+) to yield pAfcbbM. The Rca genes *cbqQ1* (AFE_3053) and *cbqQ2* (AFE_2156) were amplified from pHueAfcbbQ1 and pHueAfcbbQ2, respectively, (Tsai et al., 2015) and cloned between the *NcoI*/*HindIII* sites of the vector pCDFDuet. This resulted in plasmids pAfcbbQ1 and pAfcbbQ2, respectively. Then, the *cbbO1* (AFE_3054) and *cbbO2* (AFE_2157) were amplified from pBAD33UbAfcbbO1

and pBAD33UbAfcbbO2, respectively, (Tsai et al., 2015) and cloned into the pAfcbbQ1 and pAfcbbQ2 vectors using *NcoI* and *HindIII* restriction sites to produce pAfcRca1 and pAfcRca2. All recombinant plasmids, except pAfcRca2, were constructed by sequence and ligation-independent cloning (SLIC) as described below. pAfcRca2 was constructed by the traditional digestion ligation cloning method. The primers and their sequences are listed in **Supplementary Table S1**.

Sequence and Ligation-Independent Cloning (SLIC)

Six micrograms of vector were digested with restriction enzymes. Isolation and gel purification of the digested vector were carried out using Gene-Spin™ Miniprep Purification Kit (PROTECH, Taiwan) and Gene-Spin™ 1-4-3 DNA Purification Kit (PROTECH, Taiwan), respectively. Inserts were amplified using *Taq* DNA polymerase. For the iPCR insert, the PCR product was heated to 95°C for 5 min in a water bath for denaturation, followed by slow cooling at room temperature for 1 h for renaturation (Li and Elledge, 2007). One microgram of the vector and one microgram of the inserts were treated separately with 0.5 U of T4 DNA polymerase in T4 buffer (NEB) plus BSA in a 20 μl reaction at room temperature for 30 min (Li and Elledge, 2007). The reaction was stopped by adding 10% (v/v) of 10 mM dCTP and was then kept on ice. The annealing reaction, typically 10 μl, containing an appropriate amount of insert and vector, 1× ligation buffer (NEB), and water, was carried out at 37°C for 30 min, and then the reaction mixture was kept on ice. Finally, *E. coli* cells were transformed using a chemical transformation method (Li and Elledge, 2007).

Digestion-Ligation Cloning

Six micrograms of vector and insert were prepared by amplification using Q5 DNA polymerase. First, the vector and insert were digested with two different restriction enzymes at 37°C for 2 h. Agarose gel electrophoresis was run with the digested DNA and gel purification was conducted to isolate the DNA using the Gene-Spin™ 1-4-3 DNA purification Kit. DNA ligation was then carried out with an appropriate amount of vector and insert using T4 DNA ligase (NEB) and 1× T4 DNA ligase buffer in a 20 μl reaction at 4°C overnight. Finally, *E. coli* cells were transformed using a chemical transformation method (Sambrook et al., 1989).

Culture Media and Conditions

The strains used for fermentation experiments were grown anaerobically at 37°C and then stirred at 200 rpm in fresh 25-mL M9 defined medium containing 111 mM glucose. An anaerobic culture environment was achieved in a sealed serum bottle. A rubber stopper was used to seal the bottle, covered with an aluminum cap, and subjected to heat autoclaving for 20 min.

The initial OD₆₀₀ was adjusted to 0.05. The pH was adjusted to 8 at fermentation times of 0, 8, and 24 h using 2N NaOH. The working concentrations of streptomycin, chloramphenicol, kanamycin, and ampicillin were 50, 34, 50, and 50 μg/mL,

TABLE 1 | List of bacteria strains and plasmids used in this study.

Name	Description	Ref.
Bacterial strains		
<i>E. coli</i> BL21 (DE3)	F ⁻ , <i>dcm</i> , <i>ompT</i> , <i>gal</i> , <i>lon</i> , <i>hsdS</i> _B (rB ⁻ , mB ⁻), λ(DE3[<i>lacI</i> , <i>lacUV5-T7 gene 1</i> , <i>ind1</i> , <i>sam7</i> , <i>nin5</i>])	Lab stock
<i>E. coli</i> DH5α	F ⁻ <i>endA1</i> <i>glnV44</i> <i>thi-1</i> <i>recA1</i> <i>relA1</i> <i>gyrA96</i> <i>deoR</i> <i>nupG</i> <i>purB20</i> φ80d <i>lacZ</i> ΔM15 Δ(<i>lacZYA-argF</i>)U169, <i>hsdR17</i> (r _K ⁻ m _K ⁺), λ ⁻	Lab stock
<i>E. coli</i> MZLF	<i>E. coli</i> BL21(DE3) Δ <i>zwf</i> ::FRT <i>ldh</i> ::FRT <i>frd</i> ::FRT	Yang et al., 2016
<i>E. coli</i> MZLFA	MZLF harboring pBAD-his6- <i>prkA</i> -pACYC184 and <i>rbclS</i> -pET30a(+)	This study
Plasmids		
pBAD-his6- <i>prkA</i> -pACYC184	Recombinant plasmid carries <i>prkA</i> gene (derived from <i>Synechococcus</i> PCC7942) for the overexpression of phosphoribulokinase (PrkA) under the control of P _{BAD} .	Parikh et al., 2006
<i>rbclS</i> -pET30a(+)	Recombinant plasmid carries <i>rbclS</i> gene (originated from <i>Synechococcus</i> PCC6301) for the overexpression of engineered RuBisCO under the control of P _{T7}	Parikh et al., 2006
pLOI295	Recombinant plasmid carries <i>pdv</i> and <i>adhB</i> genes (derived from <i>Zymomonas mobilis</i>) for overexpression of Pdc-based carbon tap valve under the control of P _{lac}	Hespell et al., 1996
pET30b <i>AfcbbLS</i>	Recombinant plasmid carries <i>cbmLS</i> gene (originated from <i>A. ferrooxidans</i> ATCC 23270) for overexpression of RuBisCO under the control of P ₇ .	Tsai et al., 2015
pAfcbbM	Recombinant plasmid carries <i>cbmM</i> gene (AFE_2155) for overexpression of RuBisCO under the control of P ₇ .	This study
pAfcbbQ1	The RuBisCO activase gene <i>cbqQ1</i> (originated from <i>A. ferrooxidans</i> ATCC 23270) fused with the His ₆ -ubiquitin fragment at the native N termini, was amplified from pHueAfcbbQ1 and cloned into the vector pCDFDuet-1 with <i>NcoI</i> / <i>HindIII</i> sites.	This study
pAfcbbQ2	The RuBisCO activase gene <i>cbqQ2</i> (originated from <i>A. ferrooxidans</i> ATCC 23270) fused with the His ₆ -ubiquitin fragment at the native N termini, was amplified from pHueAfcbbQ2 and cloned into the vector pCDFDuet-1 with <i>NcoI</i> / <i>HindIII</i> sites.	This study
pAfcRca1	The gene <i>cbbO1</i> (AFE_3054) was amplified from pBAD33UbAfcbbO1 and cloned into pAfcbbQ1 vector with <i>AsiI</i> - <i>XhoI</i>	This study
pAfcRca2	The gene <i>cbbO2</i> (AFE_2157) was amplified from pBAD33UbAfcbbO2 and cloned into pAfcbbQ2 with <i>AsiI</i> - <i>XhoI</i>	This study

respectively. The working concentration of isopropyl- β -D-1-thiogalactopyranoside (IPTG) was 0.02 mM when needed.

RuBisCO Activity Assay

RuBisCO activity was assayed by adding an appropriate amount of cell-free extract to 700 μ L of reaction mixture containing cell lysate, 50 mM HEPES buffer (pH = 8), 1 mM RuBP, 20 mM MgCl₂, 5 mM DTT, 20 mM NaHCO₃, 5 mM ATP, 1 mM EDTA, 0.2 mM NADH, 15 U 3-phosphoglycerate kinase, and 6 U of glyceraldehyde 3-phosphate dehydrogenase. Cell-free extract was subjected to carbamylation at 25°C for 15 min by incubating in a reaction mixture free of RuBP (Tseng et al., 2018). The activity assay was then initiated by adding RuBP, and the consumption of NADH was determined at 25°C by measuring the UV absorbance at 340 nm. Protein quantification was carried out using the Bradford method (Bio-Rad, United States).

Analysis of Metabolites

Cell density was measured at 600 nm using a UV-Vis spectrophotometer (Thermo Fisher Scientific, United States). Samples for calculation of extracellular metabolites were collected from the culture media followed by centrifugation for 5 min at 17,000 \times g to remove cell pellets. The supernatant was filtered through a 0.2- μ m PVDF filter before sample injection. Quantification of residual glucose and extracellular formate, acetate, ethanol, lactate, and pyruvate were determined by Thermo Scientific™ Dionex™ Ultimate 3000 LC Systems. Separation of the mixture was achieved with the HPLC column Aminex HPX-87H (Bio-Rad, United States) where detection was performed with refractive index (RI, for glucose, acetate, ethanol) and ultraviolet-visible (UV-VIS, for pyruvate, lactate, formate) detectors. The mobile phase was 5-mM H₂SO₄. The column temperature was maintained at 45°C, while the flow rate was maintained at 0.6 mL/min. Sample injection (10- μ L) was performed using an auto-sampler.

The total CO₂ production of bacterial cultures was calculated by including gaseous CO₂, dissolved CO₂, and hydrated CO₂ (Zhuang and Li, 2013). Gaseous CO₂ in the head space of serum bottles was directly measured using an IR-based diffusive spectrometer (Sentry ST303, Taiwan) (Li et al., 2015). Subsequently, dissolved CO₂ and hydrated CO₂ were calculated based on the equilibrium constants as described previously (Zhuang and Li, 2013).

Calculation of Carbon Recovery

The carbon recovery can be calculated using the following equation:

$$\text{Carbon recovery (\%)} = \frac{\text{CO}_2 + \text{formate} + \text{acetate} \times 2 + \text{ethanol} \times 2 + \text{pyruvate} \times 3 + \text{lactate} \times 3}{\text{glucose consumption} \times 6}$$

where the mols each metabolite are used in the calculation. Note that the biomass is not included.

RESULTS

Construction and Expression of RuBisCO and RuBisCO Activase

The maps and verification of pAfcbbM, pAfrca1, and pAfrca2 constructed in this study are shown in **Supplementary Figures S1, S2**, respectively. The expression of all genes in *E. coli* BL21 (DE3) was confirmed by SDS-PAGE (**Supplementary Figure S3**). UbcbbM has a theoretical molecular weight of 64.8 kDa, as shown in **Supplementary Figure S3A**. UbcbbM was found in the soluble fraction. The heterologous co-expression of the UbcbbQ1 and UbcbbO1 in *E. coli* BL21(DE3) was confirmed by SDS-PAGE. UbcbbQ1 and UbcbbO1 have theoretical molecular weights of 93.4 and 38.2 kDa, as shown in **Supplementary Figure S3B**. UbcbbQ1 was found in the soluble fraction. UbcbbO1 cannot be clearly seen in the soluble fraction, which may be due to its high molecular weight. The heterologous co-expression of UbcbbQ2 and UbcbbO2 in *E. coli* BL21(DE3) was confirmed by SDS-PAGE. UbcbbQ2 and UbcbbO2 have theoretical molecular weights of 92.2 and 37.9 kDa, as shown in **Supplementary Figure S3C**. UbcbbQ2 was found in the soluble fraction. UbcbbO2 cannot be clearly seen in the soluble fraction, which may be due to its high molecular weight.

Increases in the *in vitro* Activity of RuBisCO in the Presence of RuBisCO Activase (Rca)

Table 2 shows the specific enzyme activity of different forms of RuBisCO in cell extracts of *E. coli* BL21(DE3). Form I RuBisCO (*Synechococcus* PCC6301) exhibited specific activity of $0.3 \pm 0.2 \mu\text{mol mg}^{-1} \text{min}^{-1}$, while form I RuBisCO derived from *A. ferrooxidans* ATCC 23270 showed comparable specific activity of $0.5 \pm 0.1 \mu\text{mol mg}^{-1} \text{min}^{-1}$. Form II RuBisCO derived from *A. ferrooxidans* ATCC 23270 showed specific activity of $0.5 \pm 0.2 \mu\text{mol mg}^{-1} \text{min}^{-1}$.

TABLE 2 | Specific activities of RuBisCO with RuBisCO activase (Rca) in *E. coli* BL21(DE3) crude lysate^a.

Sample ^b	Specific Activity of RuBisCO in crude lysate ^c
	$\mu\text{mol mg}^{-1} \text{min}^{-1}$
rbclS	0.3 ± 0.2
AfcbbLS	0.5 ± 0.1
AfcbbM	0.5 ± 0.2
rbclS+ Rca1	1.2 ± 0.3
AfcbbLS+ Rca1	2.2 ± 0.5
AfcbbM+ Rca2	2.6 ± 0.5

^a IPTG was supplemented (final concentration = 0.02 mM) for RuBisCO and RuBisCO activase (Rca) expression when OD₆₀₀ of bacterial cultures reached 0.4. RuBisCO and Rca were separately expressed in *E. coli* BL21(DE3). Protein quantification was carried out using the Bradford method.

^b rbclS represents form I RuBisCO originated from *Synechococcus* PCC6301. AfcbbLS and AfcbbM are form I and form II RuBisCOs originated from *A. ferrooxidans* ATCC 23270. Rca1 and Rca2 are type I and II RuBisCO activases originated from *A. ferrooxidans* ATCC 23270.

^c Errors represent standard deviation with n = 3.

Consistent with previous literature (Tsai et al., 2015), the specific activity of form I RuBisCO (from *A. ferrooxidans*) was increased by adding a second cell lysate containing overexpressed Rca1, and was increased to $2.2 \pm 0.5 \mu\text{mol mg}^{-1} \text{min}^{-1}$ (Table 2). Similarly, Rca2 also increased the specific activity of form II RuBisCO (from *A. ferrooxidans*) to $2.6 \pm 0.5 \mu\text{mol mg}^{-1} \text{min}^{-1}$. Surprisingly, form I Rca derived from *A. ferrooxidans* also enhanced the specific activity of form I RuBisCO derived from *Synechococcus* PCC6301 and reached $1.2 \pm 0.3 \mu\text{mol mg}^{-1} \text{min}^{-1}$ (Table 2).

Co-expression of RuBisCO Activase (Rca) Enhances Total Metabolite Yields

Figure 1A depicts the metabolism of the RuBisCO-based engineered *E. coli*, while Figure 1B shows the schematic of how Rca relieves the *in vivo* RuBP inhibition of RuBisCO. The results shown in Figure 2A for rbcLS, AfcbbLS, and AfcbbM indicate total metabolite yields in the range of 1.5 to 1.7 mol/molglucose, which are not significantly different than observed yields in previous study (Tseng et al., 2018). When Rca was co-expressed with the RuBisCO-based engineered pathway that was equipped with a matching form of RuBisCO, the total metabolite yields of the strains with form I RuBisCO and Rca were found to be close to 2 ($2.0 \pm 0.1 \text{ mol}_{(\text{ethanol}+\text{acetate}+\text{pyruvate})}/\text{mol}_{\text{glucose}}$ for rbcLS and $1.9 \pm 0.1 \text{ mol}_{(\text{ethanol}+\text{acetate}+\text{pyruvate})}/\text{mol}_{\text{glucose}}$ for AfcbbLS). A strain with form II RuBisCO with Rca2 exceeded 2 and reached

$2.2 \pm 0.2 \text{ mol}_{(\text{ethanol}+\text{acetate}+\text{pyruvate})}/\text{mol}_{\text{glucose}}$ (*p*-values are less than 0.05 for three pairs regarding the Rca co-expression). As shown in Figure 2B, the co-expression of Rca1 decreased glucose consumption from 41 and 44 mM down to 29 and 34 mM for rbcLS and AfcbbLS, respectively. In contrast, the co-expression of Rca2 does not affect glucose consumption (Figure 2B). Figure 2C indicates that the co-expression of Rca has the effect of cascading the carbon flow to the conventional metabolites so that the carbon recovery significantly increased from 80, 84, and 73% to 93, 92, and 100% for rbcLS, AfcbbLS, and AfcbbM, respectively.

Introduction of the Pdc-Based Pathway Elevates Both the Performance of the *in situ* CO₂ Recycling and Glucose Consumption of the *E. coli* Strain Harboring Form I RuBisCO

In our previous study (Tseng et al., 2018), the Pdc-based pathway (ethanol production pathway) consisting of pyruvate carboxylase (Pdc) and alcohol dehydrogenase (AdhB) (Hespell et al., 1996), (referred to as Pdc in this study) was found to effectively increase glucose consumption by creating ATP demand. A significant result of the Tseng et al. (2018) study was that glucose was diverted to the RuBisCO-based engineered pathway during elevated glucose consumption. Therefore, the performance of *in situ* CO₂ recycling was accordingly enhanced (Tseng et al., 2018). In this study, Pdc

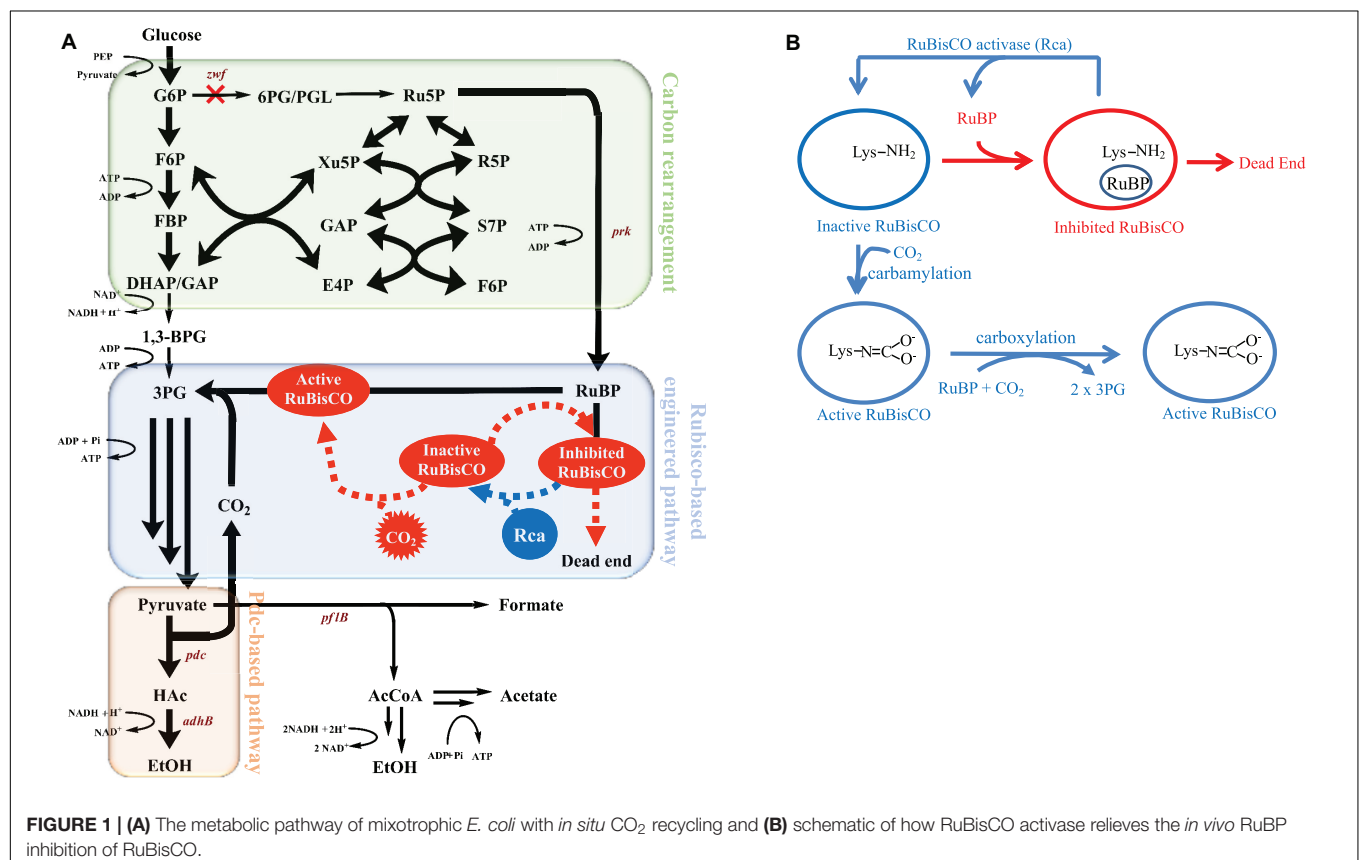
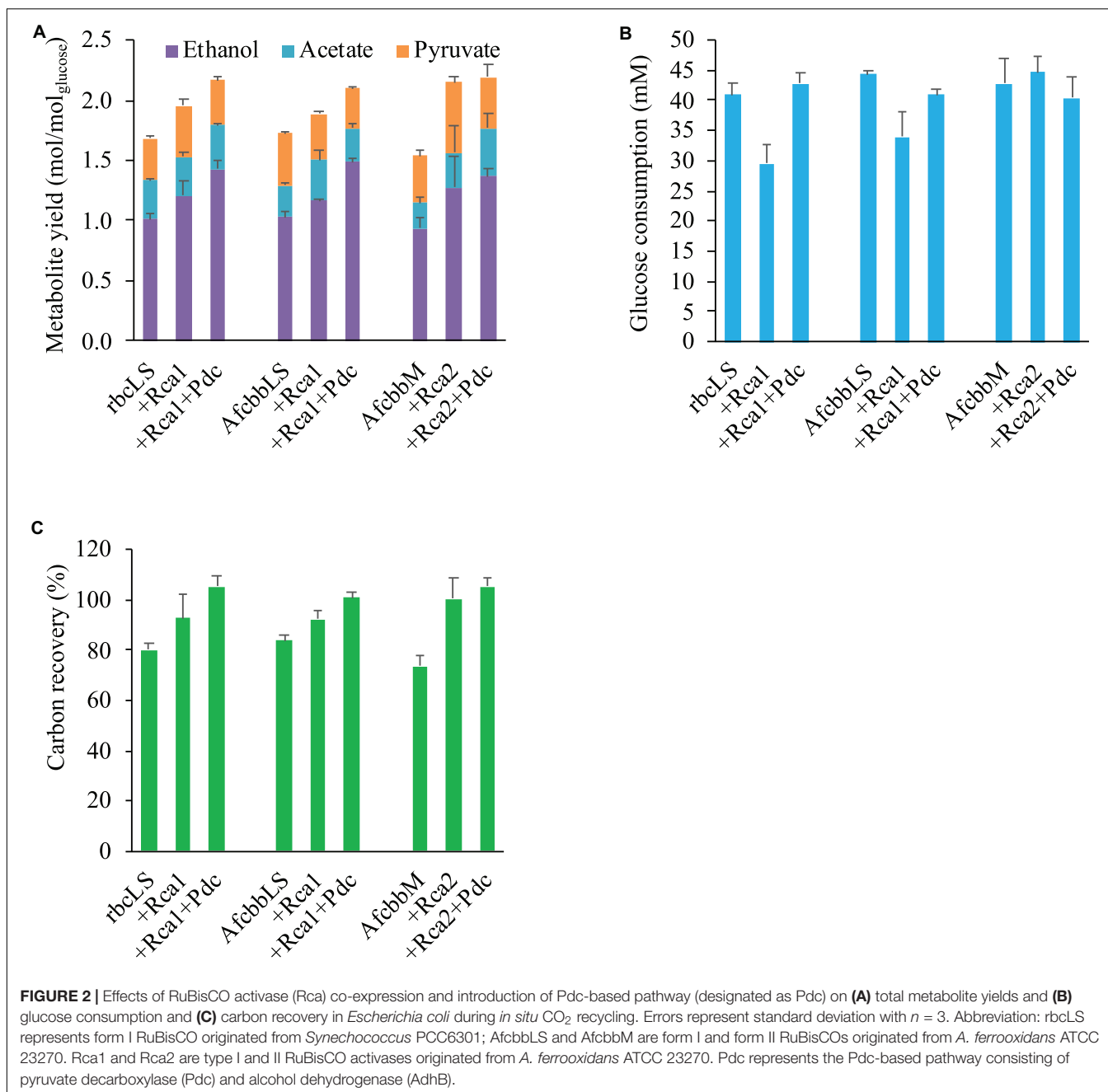
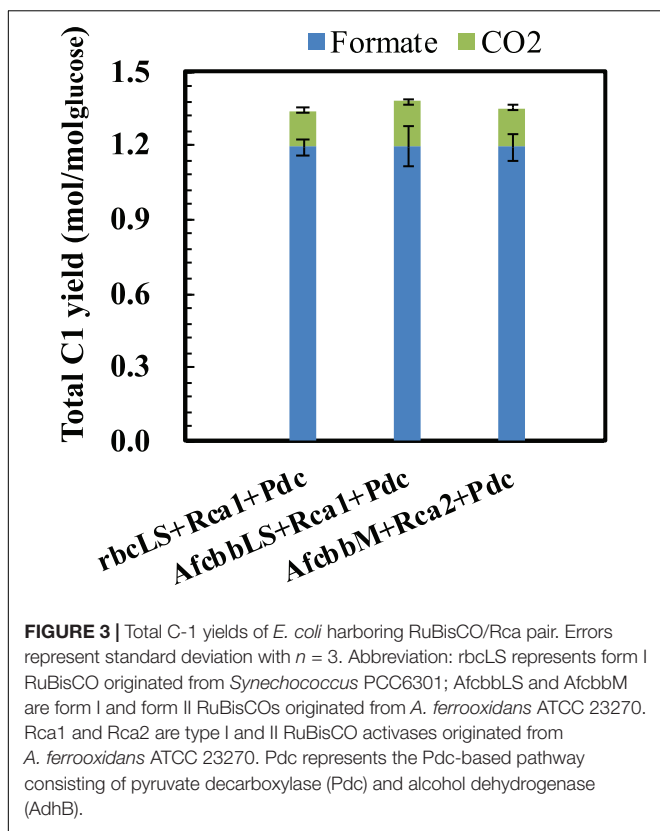


FIGURE 1 | (A) The metabolic pathway of mixotrophic *E. coli* with *in situ* CO₂ recycling and **(B)** schematic of how RuBisCO activase relieves the *in vivo* RuBP inhibition of RuBisCO.



was introduced in the A+Rca system. **Figure 2A** shows that the introduction of Pdc substantially improves the performance of *in situ* CO₂ recycling in RuBisCO-based *E. coli* harboring form I RuBisCO. The total metabolite yields of rbcLS+Rca1+Pdc and AfcbbLS+Rca1+Pdc were 2.2 ± 0.1 and 2.1 ± 0.1 mol_(ethanol+acetate+pyruvate)/mol_{glucose}, which exceeded the conventional fermentation yield of 2 mol_(ethanol+acetate+pyruvate)/mol_{glucose}. The increases in total metabolite yields illustrated in **Figure 2A** were primarily due to increased ethanol yields. The high total C-2 (ethanol+acetate) yield of 1.8 mol_(ethanol+acetate)/mol_{glucose} was accompanied by a low total C-1 yield of 1.4 mol_(formate+CO₂)/mol_{glucose} (**Figure 3**),

where the C-2/C-1 ratio theoretically should be 1. In addition to increasing the total metabolite yields for the two cases with form I RuBisCO, the introduction of the Pdc-based pathway also recovered the glucose consumption back to 40 mM (**Figure 2B**) and increased the carbon recovery (**Figure 2C**) for the two cases with form I RuBisCO. When Rca was co-expressed with the RuBisCO-based engineered pathway that was equipped with a matching form of RuBisCO, the total metabolite yields of the strains with form I RuBisCO and Rca were found to be close to 2 (2.0 ± 0.1 mol_(ethanol+acetate+pyruvate)/mol_{glucose} for rbcLS and 1.9 ± 0.1 mol_(ethanol+acetate+pyruvate)/mol_{glucose} for AfcbbLS), while a strain with form II RuBisCO with Rca2 exceeded 2 and



reached $2.2 \pm 0.2 \text{ mol}_{(\text{ethanol}+\text{acetate}+\text{pyruvate})}/\text{mol}_{\text{glucose}}$ (p -values are less than 0.05 for three pairs regarding the Rca co-expression).

DISCUSSION

This study demonstrated that both form I and form II RuBisCO can be functionally expressed in *E. coli* (Table 2), which is consistent with previous studies which showed that the functional expression of bacterial Rubisco in *E. coli* is not of concern (Parikh et al., 2006; Tsai et al., 2015; Antonovsky et al., 2016; Tseng et al., 2018). The enzymatic assay of RuBisCO indicates that both form I and form II RuBisCO are subject to RuBP inhibition, but the RuBP inhibition can be relieved in the presence of Rca (Table 2). While the *in vitro* RuBP inhibition of RuBisCO shown here is consistent with a previous study (Tsai et al., 2015), this study further revealed that forms I and II RuBisCO also undergo RuBP inhibition *in vivo* because rbcLS, AfcbbLS, and AfcbbM in Figure 2A exhibit insignificant *in situ* CO₂ recycling. The *in vivo* RuBP inhibition of form I RuBisCO can be alleviated by the co-expression of form I RuBisCO activase (Rca1). This is supported by the result that rbcLS+Rca1 and AfcbbLS+Rca1 have a significant increase in total fermentation product yield (Figure 2A), resulting from the concentrated carbon flow to the RuBisCO-based engineered pathway. Thus, it is suggested that the direction of the carbon flow to the RuBisCO-based engineered pathway is driven by the high activity of Prk when the catalytic power of RuBisCO is sufficient.

The sugar phosphate, RuBP, is known as a tight binder to RuBisCO owing to its low $K_{M,RuBP}$ (McNevin et al., 2006). Therefore, high levels of intracellular CO₂ are necessary to compete with RuBP to activate RuBisCO by carbamylation. Our previous study showed that a total fermentation yield of 2.17 was achieved at a CO₂ yield of 0.8 mol/mol_{glucose}. In contrast, this study showed that high fermentation product yields (Figure 2A) can be achieved at low CO₂ yields below 0.2 mol/mol_{glucose} (Figure 3), supporting the remodel of inhibited RuBisCO by Rca.

The effectiveness of Rca co-expression for enhancing *in situ* CO₂ recycling reflects the substantial issue of *in vivo* RuBisCO inhibition. The *in vivo* RuBisCO inhibition can be overcome by introducing the Pdc-based ethanol biosynthesis pathway (Pdc) so that a significant amount of CO₂ can be produced to compete with RuBP for activating RuBisCO (Tseng et al., 2018). The *in vivo* RuBisCO inhibition can also be solved by Rca co-expression, as shown in this study. The introduction of Pdc in *E. coli* strains harboring form I RuBisCO provides compensation (Figure 2A), indicating that *in vivo* inhibition of form I RuBisCO is more complex and requires CO₂ production from the function of Pdc. In fact, the failure of formate dehydrogenase (FDH) co-expression to elevate the performance of *in situ* CO₂ recycling may simply be because CO₂ production is too low due to poor FDH activity (Tseng et al., 2018).

It should be noted that the activity of Pdc in the presence of Rca was significantly reduced as acetate and formate were significantly produced (Figure 2A). This could be attributed to the strong ATP demand created by Rca which therefore stimulates the downstream carbon flux to the native *pflB*-mediated pathway to produce acetate and formate, where acetate production is accompanied by ATP production (Schäfer et al., 1993). The trimmed activity of Pdc in the presence of Rca also led to a lower glucose consumption (approximately 40 mM, Figure 2B) compared to that (64 mM) without Rca (Tseng et al., 2018). Note that the extent to which RuBisCO is inhibited in *E. coli* could not be determined based on the activity and fermentation data.

The functional expression of Rca1 can be supported by low glucose consumption of rbcLS+Rca1 and AfcbbLS+Rca1 (Figure 2B). This can be attributed to a high ATP consumption by the Rca1 function, which negatively affects the bacterial growth (data not shown). In contrast, *in vivo* RuBP inhibition of form II RuBisCO can also be addressed with by the co-expression of form II RuBisCO activase (Rca2, Figure 2A). However, AfcbbM+Rca2 has a comparable glucose consumption (Figure 2B) and bacterial growth (data not shown) compared with those in the absence of Rca2. This indicates that reducing the *in vivo* RuBP inhibition of form II RuBisCO may be easier without a significant amount of ATP input. The difference in the ATP demand between forms I and II Rca may be attributed to the plausible role of the small subunit of RuBisCO. Large and small subunits of RuBisCO co-evolve to adapt to environmental changes. Large subunits play a role mainly in catalysis, while small subunits influence not only catalytic efficiency, but also CO₂ specificity and the assembly and stability of the L₈S₈ holoenzyme. Small subunits provide RuBisCO more flexibility to

adapt to environmental changes. For example, RuBisCO requires a repeated activation process by Rca to maintain its activity. Although the repeated activation process lowers the catalytic performance of RuBisCO, this makes Rca a good regulator to control RuBisCO activity under certain environmental conditions, such as stromal ATP/ADP ratio (Zhang and Portis, 1999). This study concurs with the above argument that the *in vivo* activity of form I RuBisCO in *E. coli* depends heavily on Rca compared to that of form II RuBisCO. The advantage of using form II RuBisCO for engineering applications is that the *in vivo* RuBP inhibition can be recovered at a low ATP demand.

In past research, it has been demonstrated that the interaction between Rca and RuBisCO comes from the same kind of bacteria (Tsai et al., 2015). In this study, we introduced form I RuBisCO from *Synechococcus* PCC6301 and form I Rca from *A. ferrooxidans* to *E. coli* MZLF. Interestingly, although RuBisCO is from a different species, Rca showed an ability to increase RuBisCO activity, both *in vitro* (Table 2) and *in vivo* (Figure 2). Either Asp82 or HK/R motif at the C-terminus of RuBisCO large subunit has been shown to be essential for *in vitro* activation of the ATPase activity of CbbQ (Tsai et al., 2015). While rbcLS lacks the Asp82 and HK/R motif, the *in vivo* effectiveness of Rca1 in regulating the activity of rbcLS was demonstrated in this study. *In vivo* interactions involving CbbO, CbbQ, and RuBisCO without the HK/R motif could be further investigated.

In summary, both form I and form II RuBisCO undergo *in vivo* RuBP inhibition. On top of the intrinsic low k_{cat} of RuBisCO, *in vivo* RuBP inhibition of RuBisCO has been shown to make apparent k_{cat} low and thus becoming a bottleneck for *in situ* CO₂ recycling in *E. coli*. The co-expression of Rca can relieve this *in vivo* RuBP inhibition. Furthermore, it is suggested that the *in vivo* RuBP inhibition of form II RuBisCO is easier to address than that of form I RuBisCO. When the catalytic power of RuBisCO is secured, the high activity of Prk plays an important role in directing carbon flow to the RuBisCO-based engineered pathway and produces high fermentation yields of 2.1–2.3 mol(ethanol+acetate+pyruvate)/mol_{glucose}.

REFERENCES

- Antonovsky, N., Gleizer, S., Noor, E., Zohar, Y., Herz, E., Barenholz, U., et al. (2016). Sugar Synthesis from CO₂ in *Escherichia coli*. *Cell* 166, 115–125.
- Ashida, H., Saito, Y., Nakano, T., Tandeau De Marsac, N., Sekowska, A., Danchin, A., et al. (2008). RuBisCO-like proteins as the enolase enzyme in the methionine salvage pathway: functional and evolutionary relationships between RuBisCO-like proteins and photosynthetic RuBisCO. *J. Exp. Bot.* 59, 1543–1554. doi: 10.1093/jxb/ern104
- Badger, M. R., and Bek, E. B. (2008). Multiple Rubisco forms in proteobacteria: their functional significance in relation to CO₂ acquisition by the CBB cycle. *J. Exp. Bot.* 59, 1525–1541. doi: 10.1093/jxb/ern297
- François, J. M., Lachaux, C., and Morin, N. (2020). Synthetic biology applied to carbon conservative and carbon dioxide recycling pathways. *Front. Bioeng. Biotechnol.* 7:446. doi: 10.3389/fbioe.2019.00446
- Gassler, T., Sauer, M., Gasser, B., Egermeier, M., Troyer, C., Causon, T., et al. (2019). The industrial yeast *Pichia pastoris* is converted from a heterotroph into an autotroph capable of growth on CO₂. *Nat. Biotechnol.* 38, 210–216. doi: 10.1038/s41587-019-0363-0

DATA AVAILABILITY STATEMENT

The raw data supporting the conclusions of this article will be made available by the authors, without undue reservation.

AUTHOR CONTRIBUTIONS

J-JP designed research, carried out experiments, and analyzed data. J-SS analyzed data and wrote the manuscript. S-YL conceived and designed research, analyzed data, and wrote the manuscript. All authors read and approved the final manuscript.

FUNDING

This work was funded by the Ministry of Science and Technology Taiwan, MOST-106-2221-E-005-058-MY3, MOST-108-2628-E-005-002-MY3, and the Ministry of Education, Taiwan, R.O.C. under the Higher Education Sprout Project.

ACKNOWLEDGMENTS

The authors thank Prof. Oliver Mueller-Cajar of Biological Sciences School at Nanyang Technological University, Singapore for his generous gifts of pET30bAfcbbLS, pHueAfcbbM, pHueAfcbbQ1, pHueAfcbbQ2, pBAD33UbAfcbbO1, and pBAD33UbAfcbbO2. The authors thank Prof. Richard Parnas of Chemical & Biomolecular Engineering at the University of Connecticut, United States for proofreading the manuscript.

SUPPLEMENTARY MATERIAL

The Supplementary Material for this article can be found online at: <https://www.frontiersin.org/articles/10.3389/fbioe.2020.543807/full#supplementary-material>

- Hespell, R. B., Wyckoff, H., Dien, B. S., and Bothast, R. J. (1996). Stabilization of pet operon plasmids and ethanol production in *Escherichia coli* strains lacking lactate dehydrogenase and pyruvate formate-lyase activities. *Appl. Environ. Microbiol.* 62, 4594–4597. doi: 10.1128/aem.62.12.4594-4597.1996
- Li, M. Z., and Elledge, S. J. (2007). Harnessing homologous recombination in vitro to generate recombinant DNA via SLIC. *Nat. Methods* 4, 251–256. doi: 10.1038/nmeth1010
- Li, Y.-H., Ou-Yang, F.-Y., Yang, C.-H., and Li, S.-Y. (2015). The coupling of glycolysis and the Rubisco-based pathway through the non-oxidative pentose phosphate pathway to achieve low carbon dioxide emission fermentation. *Bioresour. Technol.* 187, 189–197. doi: 10.1016/j.biortech.2015.03.090
- McNevin, D., Von Caemmerer, S., and Farquhar, G. (2006). Determining RuBisCO activation kinetics and other rate and equilibrium constants by simultaneous multiple non-linear regression of a kinetic model. *J. Exp. Bot.* 57, 3883–3900. doi: 10.1093/jxb/erl156
- Mueller-Cajar, O. (2017). The diverse AAA+ Machines that repair inhibited rubisco active sites. *Front. Mol. Biosci.* 4:31. doi: 10.3389/fmolb.2017.00031
- Nielsen, C. J., Herrmann, H., and Weller, C. (2012). Atmospheric chemistry and environmental impact of the use of amines in carbon capture and storage (CCS). *Chem. Soc. Rev.* 41, 6684–6704. doi: 10.1039/c2cs35059a

- Parikh, M. R., Greene, D. N., Woods, K. K., and Matsumura, I. (2006). Directed evolution of RuBisCO hypermorphs through genetic selection in engineered *E. coli*. *Protein Eng. Des. Sel.* 19, 113–119. doi: 10.1093/protein/gzj010
- Parry, M. A. J., Keys, A. J., Madgwick, P. J., Carmo-Silva, A. E., and Andralojc, P. J. (2008). Rubisco regulation: a role for inhibitors. *J. Exp. Bot.* 59, 1569–1580. doi: 10.1093/jxb/ern084
- Salvucci, M. E., Portis, A. R., and Ogren, W. L. J. P. R. (1985). A soluble chloroplast protein catalyzes ribulosebiphosphate carboxylase/oxygenase activation in vivo. *Photosynth. Res.* 7, 193–201. doi: 10.1007/bf00037012
- Sambrook, J., Fritsch, E. F., and Maniatis, T. (1989). *Molecular Cloning: A Laboratory Manual*. Cold Spring Harbor, NJ: Cold spring harbor laboratory press.
- Schäfer, T., Selig, M., and Schönheit, P. (1993). Acetyl-CoA synthetase (ADP forming) in archaea, a novel enzyme involved in acetate formation and ATP synthesis. *Arch. Microbiol.* 159, 72–83. doi: 10.1007/bf00244267
- Somerville, C., Portis, A. R., and Ogren, W. L. (1982). A mutant of *Arabidopsis thaliana* which lacks activation of RuBP carboxylase in vivo. *Plant Physiol.* 70, 381–387. doi: 10.1104/pp.70.2.381
- Tabita, F. R., Satagopan, S., Hanson, T. E., Kreel, N. E., and Scott, S. S. (2008). Distinct form I, II, III, and IV Rubisco proteins from the three kingdoms of life provide clues about Rubisco evolution and structure/function relationships. *J. Exp. Bot.* 59, 1515–1524. doi: 10.1093/jxb/erm361
- Tsai, Y.-C. C., Lapina, M. C., Bhushan, S., and Mueller-Cajar, O. (2015). Identification and characterization of multiple rubisco activases in chemoautotrophic bacteria. *Nat. Commun.* 6:8883.
- Tsai, Y.-C. C., Ye, F., Liew, L., Liu, D., Bhushan, S., Gao, Y.-G., et al. (2020). Insights into the mechanism and regulation of the CbbQO-type Rubisco activase, a MoxR AAA+ ATPase. *Proc. Natl. Acad. Sci. U.S.A.* 117, 381–387. doi: 10.1073/pnas.1911123117
- Tseng, I. T., Chen, Y.-L., Chen, C.-H., Shen, Z.-X., Yang, C.-H., and Li, S.-Y. (2018). Exceeding the theoretical fermentation yield in mixotrophic Rubisco-based engineered *Escherichia coli*. *Metab. Eng.* 47, 445–452. doi: 10.1016/j.ymben.2018.04.018
- Yang, C.-H., Liu, E.-J., Chen, Y.-L., Ou-Yang, F.-Y., and Li, S.-Y. (2016). The comprehensive profile of fermentation products during in situ CO₂ recycling by Rubisco-based engineered *Escherichia coli*. *Microb. Cell Fact.* 15, 1–10.
- Zhang, N., and Portis, A. R. (1999). Mechanism of light regulation of Rubisco: a specific role for the larger Rubisco activase isoform involving reductive activation by thioredoxin-f. *Proc. Natl. Acad. Sci. U.S.A.* 96, 9438–9443. doi: 10.1073/pnas.96.16.9438
- Zhuang, Z.-Y., and Li, S.-Y. (2013). Rubisco-based engineered *Escherichia coli* for in situ carbon dioxide recycling. *Bioresour. Technol.* 150, 79–88. doi: 10.1016/j.biortech.2013.09.116

Conflict of Interest: The authors declare that the research was conducted in the absence of any commercial or financial relationships that could be construed as a potential conflict of interest.

Copyright © 2020 Pang, Shin and Li. This is an open-access article distributed under the terms of the Creative Commons Attribution License (CC BY). The use, distribution or reproduction in other forums is permitted, provided the original author(s) and the copyright owner(s) are credited and that the original publication in this journal is cited, in accordance with accepted academic practice. No use, distribution or reproduction is permitted which does not comply with these terms.